TABLE 6. Distribution of Genotype of ARMS2 A69S, CFH I62 V, and CFH Y402 in Patients With vs Without Reticular Pseudodrusen in Late Age-Related Macular Degeneration

	Reticular Pseudodrusen (+) (n=28)					Reticular Pseudodrusen (-) (n=177)					
	Genotype, n (%)			Allele, n (%)		Genotype, n (%)			Allele, n (%)		P[a]
ARMS2 A69S	GG	GT	TT	G	T	GG	GT	TT	G	T	
	1 (3.6)	10 (35.7)	17 (60.7)	12 (21.4)	44 (78.6)	33 (18.7)	76 (42.9)	68 (38.4)	142 (40.1)	212 (59.9)	.007
CFH I62 V	AA	AG	GG	A	G	AA	AG	GG	A	G	
	4 (14.3)	4 (14.3)	20 (71.4)	12 (21.4)	44 (78.6)	16 (9.1)	49 (27.8)	111 (63.1)	81 (23.0)	271 (77.0)	.865
CFH Y402	CC	CT	TT	C	T	CC	CT	TT	C	T	
	1 (3.6)	6 (21.4)	21 (75.0)	8 (14.3)	48 (85.7)	7 (4.0)	45 (25.4)	125 (70.6)	59 (16.7)	295 (83.3)	.845

[a]P value with 2 × 2 table of allele χ^2 test for its exact counterpart.

In the current study, reticular pseudodrusen prevalence was high in eyes with RAP or geographic atrophy, consistent with previous reports.[5,6] Therefore, reticular pseudodrusen may represent a hallmark or adverse effect associated with the pathology of RAP and geographic atrophy. In contrast, reticular pseudodrusen was rarely found in PCV patients (2%). To our knowledge, this is the first report on reticular pseudodrusen prevalence in PCV patients.

Literature suggests an association between AMD and polymorphisms in the *CFH* gene.[15-19,24] The Y402H and I62 V variants, in particular, have been specifically reported to be associated with AMD.[15-19,24] In a Japanese cohort, we have previously shown that both *CFH* Y402H and I62 V are associated with AMD.[19] The Beaver Dam Eye Study showed a higher prevalence of reticular pseudodrusen in participants carrying the Y402H mutation of the C allele, which is associated with an increased risk of AMD.[8] In contrast, Smith and associates reported that this *CFH* variant was significantly associated with absence of reticular pseudodrusen.[25] We found no association between reticular pseudodrusen and *CFH* Y402H in patients with late AMD. As the frequency of the Y402H C allele is very low in the Asian population,[34-36] it may be difficult to show a significant difference. In contrast, I62 V is more suitable for an association study focusing on the *CFH* gene in Japanese people, because its minor allele frequency is approximately 40%.[19,24] However, in the current study, we found no association between I62 V and reticular pseudodrusen.

The A69S variant of the *ARMS2* gene is also associated with AMD; this association was reported in white and Asian subjects.[19-23,37-42] Smith and associates reported that the *ARMS2* A69S allele increases the risk for reticular pseudodrusen.[25] In the current study, the T-allele frequencies of the *ARMS2* A69S were higher in reticular pseudodrusen patients, which suggests that the A69S polymorphism contributed to reticular pseudodrusen development. Although we reported higher T-allele frequencies for *ARMS2* A69S than Smith and associates,[25] the risk-allele frequency in patients without reticular pseudodrusen was similar to that reported in previous studies on Japanese patients.[43,44] The finding that both the *ARMS2* risk allele and reticular pseudodrusen apparently lead to late AMD may suggest a common mechanism. Although the function of *ARMS2* is unknown, Fritsche and associates showed that *ARMS2* was expressed in the ellipsoid region of the photoreceptor inner segments.[39] Despite the controversial localization of reticular pseudodrusen, several researchers have shown that reticular pseudodrusen location corresponds to that of abnormal material above the RPE.[9,45] Thus, *ARMS2* expression may colocalize with reticular pseudodrusen, raising the possibility that *ARMS2* may play a role in the formation of reticular pseudodrusen. Meanwhile, other reports suggest that the reticular pattern is related to impaired choroidal filling, as observed in our subjects, and may involve the RPE, choriocapillaris, and inner choroid.[3,14,46] Querques and associates proposed that derangement of the RPE attributable to underlying atrophy and fibrosis of the choroid might lead to the accumulation of photoreceptor outer segments above the RPE.[28] Kertvely and associates showed that *ARMS2* gene expression localized primarily to the intercapillary area of the choroid.[47] Further investigations are required on the histology of reticular pseudodrusen and the locations and functions of *ARMS2* during the course of AMD.

Our study had several limitations. First, this study was retrospective, and the imaging protocol was not standardized. Second, the sample size was relatively small compared with that used in other prevalence and genetic studies, and we included several disease types. Third, a single grader subjectively evaluated image quality. When the same researcher evaluated it again, intra-observer agreement was high. Fourth, our results show that the prevalence of reticular pseudodrusen was high in patients with RAP or geographic atrophy, but the small sample size of these patients prevented us from establishing this trend. Finally, the techniques used here may have failed to identify reticular pseudodrusen in eyes in which reticular pseudodrusen was present only on the nasal side of the optic disc.[13] Furthermore, some patients with

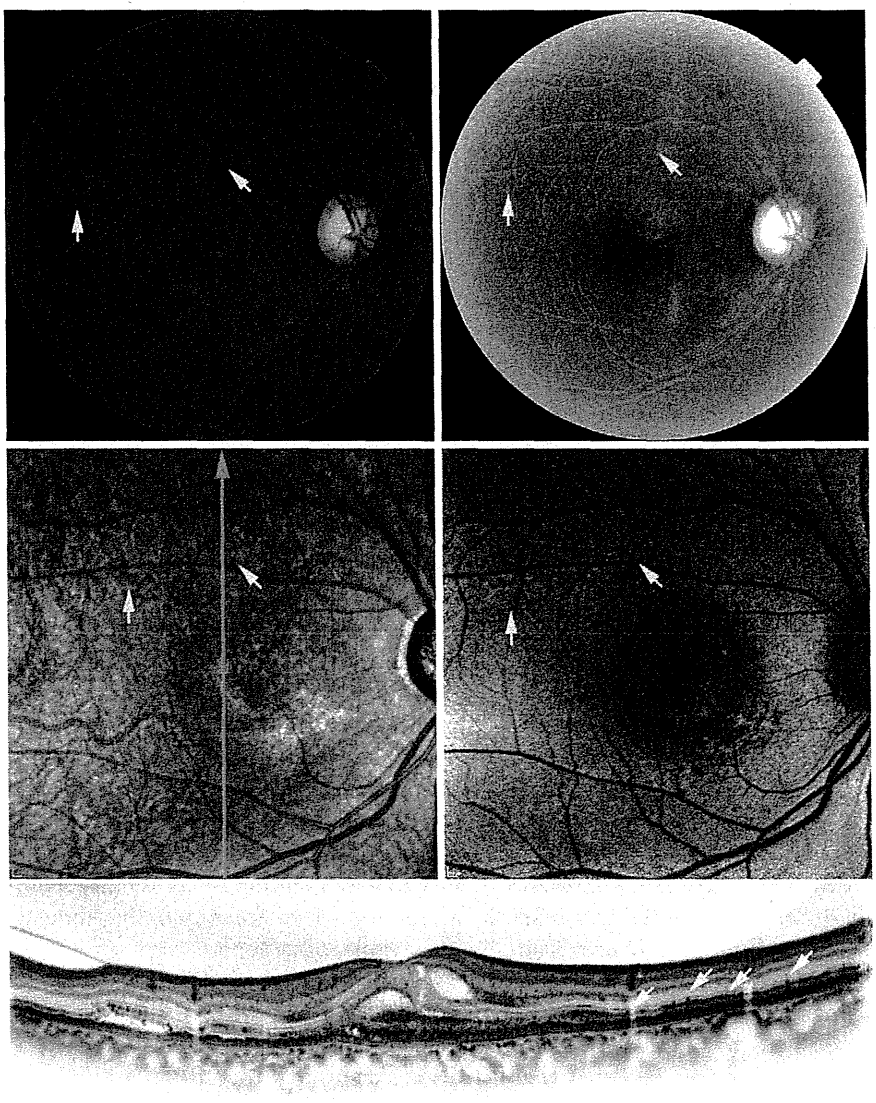

FIGURE 2. Images of a patient with neovascular age-related macular degeneration and reticular pseudodrusen. (Top row, left) Color fundus photography. (Top row, right) Blue channel of contrast-enhanced color fundus photography. (Second row, left) Infrared reflectance imaging. (Second row, right) Fundus autofluorescence imaging. (Bottom) Spectral-domain optical coherence tomography (vertical B-scan thorough the fovea in the direction of the green arrow in Second row, left). Reticular pattern is visible in each imaging (arrows), but it may be difficult to make a diagnosis of reticular pseudodrusen using only 1 imaging method.

bilateral CNV may have had reticular pseudodrusen before CNV development.

In conclusion, reticular pseudodrusen was found in 14% of patients with newly diagnosed late AMD using multimodal imaging. About half of the patients with reticular pseudodrusen had bilateral late AMD. Moreover, there was an association between reticular pseudodrusen and the *ARMS2* gene. Further epidemiologic or genetic studies will deepen our understanding of the clinical significance of reticular pseudodrusen.

ALL AUTHORS HAVE COMPLETED AND SUBMITTED THE ICMJE FORM FOR DISCLOSURE OF POTENTIAL CONFLICTS OF INTEREST and none were reported. Publication of this article was supported in part by the Grant-in-Aid for Scientific Research (21791679) from the Japan Society for the Promotion of Science (JSPS), Tokyo, Japan. Contributions of authors: conception and design (S.O.); analysis and interpretation (N.U.A., S.O., I.N.); writing the manuscript (N.U.A., S.O.); critical revision of the manuscript (S.O., K.Y., A.T., A.O., N.Y.); final approval of the article (N.U.A., S.O., I.N., K.Y., A.T., A.O., N.Y.); data collection (N.U.A., I.N., K.Y.); statistical expertise (N.U.A., S.O., I.N.); obtaining funding (S.O., K.Y., N.Y.); literature search (N.U.A., S.O.); and technical support (I.N., K.Y.).

REFERENCES

1. Mimoun G, Soubrane G, Coscas G. Les drusen maculaires. *J Fr Ophtalmol* 1990;13(10):511–530.
2. Klein R, Davis MD, Magli YL, et al. The Wisconsin age-related maculopathy grading system. *Ophthalmology* 1991; 98(7):1128–1134.
3. Arnold JJ, Sarks SH, Killingsworth MC, et al. Reticular pseudodrusen. A risk factor in age-related maculopathy. *Retina* 1995;15(3):183–191.
4. Cohen SY, Dubois L, Tadayoni R, et al. Prevalence of reticular pseudodrusen in age-related macular degeneration with newly diagnosed choroidal neovascularization. *Br J Ophthalmol* 2007;91(3):354–359.
5. Sarks J, Arnold J, Ho I-V, Sarks S, Killingsworth M. Evolution of reticular pseudodrusen. *Br J Ophthalmol* 2011;95(7):979–985.
6. Pumariega NM, Smith RT, Sohrab MA, LeTien V, Souied EH. A prospective study of reticular macular disease. *Ophthalmology* 2011;118(8):1619–1625.
7. Schmitz-Valckenberg S, Alten F, Steinberg JS, et al. Reticular drusen associated with geographic atrophy in age-related macular degeneration. *Invest Ophthalmol Vis Sci* 2011;52(9):5009–5015.
8. Klein R, Meuer SM, Knudtson MD, Iyengar SK, Klein BEK. The epidemiology of retinal reticular drusen. *Am J Ophthalmol* 2008;145(2):317–326.
9. Zweifel SA, Spaide RF, Curcio CA, et al. Reticular pseudodrusen are subretinal drusenoid deposits. *Ophthalmology* 2010;117(2):303–312.
10. Zweifel SA, Imaura Y, Spaide TC, Fujiwara T, Spaide RF. Prevalence and significance of subretinal drusenoid deposits (reticular pseudodrusen) in age-related macular degeneration. *Ophthalmology* 2010;117(9):1775–1781.
11. Lois N, Owens SL, Coco R, Hopkins J, Fitzke FW, Bird AC. Fundus autofluorescence in patients with age-related macular degeneration and high risk of visual loss. *Am J Ophthalmol* 2002;133(3):341–349.
12. Bindewald A, Bird AC, Dandekar SS, et al. Classification of fundus autofluorescence patterns in early age-related macular disease. *Invest Ophthalmol Vis Sci* 2005;46(9):3309–3314.
13. Smith RT, Chan JK, Busuoic M, et al. Autofluorescence characteristics of early, atrophic, and high-risk fellow eyes in age-related macular degeneration. *Invest Ophthalmol Vis Sci* 2006; 47(12):5495–5504.
14. Smith RT, Sohrab MA, Busuioc M, Barile G. Reticular macular disease. *Am J Ophthalmol* 2009;148(5):733–743.
15. Hageman GS, Anderson DH, Johnson LV, et al. A common haplotype in the complement regulatory gene factor H (HF1/CFH) predisposes individuals to age-related macular degeneration. *PNAS* 2005;102(20):7227–7232.
16. Klein RJ, Zeiss C, Chew EY, et al. Complement factor H polymorphism in age-related macular degeneration. *Science* 2005; 308(5720):385–389.
17. Haines JL, Hauser MA, Schmidt S, et al. Complement factor H variant increases the risk of age-related macular degeneration. *Science* 2005;308(5720):419–421.
18. Edwards AO, Ritter R 3rd, Abel KJ, Manning A, Panhuysen C, Farrer LA. Complement factor H polymorphism and age-related macular degeneration. *Science* 2005; 308(5720):421–424.
19. Hayashi H, Yamashiro K, Gotoh N, et al. CFH and ARMS2 variations in age-related macular degeneration, polypoidal choroidal vasculopathy, and retinal angiomatous proliferation. *Invest Ophthalmol Vis Sci* 2010;51(11):5914–5919.
20. Schmidt S, Hauser MA, Scott WK, et al. Cigarette smoking strongly modifies the association of LOC387715 and age-related macular degeneration. *Am J Hum Genet* 2006;78(5): 852–864.
21. Dewan A, Liu M, Hartman S, et al. HTRA1 promoter polymorphism in wet age-related macular degeneration. *Science* 2006;314(5801):989–992.
22. Yang Z, Camp NJ, Sun H, et al. A variant of the HTRA1 gene increases susceptibility to age-related macular degeneration. *Science* 2006;314(5801):992–993.
23. Rivera A, Fisher SA, Fritsche LG, et al. Hypothetical LOC387715 is a second major susceptibility gene for age-related macular degeneration, contributing independently of complement factor H to disease risk. *Hum Mol Genet* 2005;14(21):3227–3236.
24. Mori K, Horie-Inoue K, Gehlbach PL, et al. Phenotype and genotype characteristics of age-related macular degeneration in a Japanese population. *Ophthalmology* 2010;117(5):928–938.
25. Smith RT, Merriam JE, Sohrab MA, et al. Complement factor H 402H variant and reticular macular disease. *Arch Ophthalmol* 2011;129(8):1061–1066.
26. Yannuzzi LA, Negrao S, Iida T, et al. Retinal angiomatous proliferation in age-related macular degeneration. *Retina* 2001;21(5):416–434.
27. Arnold JJ, Quaranta M, Soubrane G, Sarks SH, Coscas G. Indocyanine green angiography of drusen. *Am J Ophthalmol* 1997;124(3):344–356.
28. Querques G, Querques L, Forte R, Massamba N, Coscas F, Souied EH. Choroidal changes associated with reticular pseudodrusen. *Invest Ophthalmol Vis Sci* 2012;53(3):1258–1263.
29. Maruko I, Iida T, Saito M, Nagayama D, Saito K. Clinical characteristics of exudative age-related macular degeneration in Japanese patients. *Am J Ophthalmol* 2007;144(1):15–22.
30. Oshima Y, Ishibashi T, Murata T, Tahara Y, Kiyohara Y, Kubota T. Prevalence of age-related maculopathy in a retrospective Japanese population: the Hisayama study. *Br J Ophthalmol* 2001;85(10):1153–1157.
31. Klein R, Chou CF, Klein BE, Zhang X, Meuer SM, Saaddine JB. Prevalence of age-related macular degeneration in the US population. *Arch Ophthalmol* 2011;129(1):75–80.
32. Klein R, Klein BE, Linton KL. Prevalence of age-related maculopathy. The Beaver Dam Eye Study. *Ophthalmology* 1992;99(6):933–943.
33. Lee MY, Yoon J, Ham DI. Clinical characteristics of reticular pseudodrusen in Korean patients. *Am J Ophthalmol* 2012; 153(3):530–535.
34. Gotoh N, Yamada R, Hiratani H, et al. No association between complement factor H gene polymorphism and exudative age-related macular degeneration in Japanese. *Hum Genet* 2006;120(1):139–143.
35. Fuse N, Miyazawa A, Mengkegale M, et al. Polymorphisms in Complement Factor H and Hemicentin-1 genes in a Japanese population with dry-type age-related macular degeneration. *Am J Ophthalmol* 2006;142(6):1074–1076.
36. Kim NR, Kang JH, Kwon OW, Lee SJ, Oh JH, Chin HS. Association between complement factor H gene polymorphisms

and neovascular age-related macular degeneration in Koreans. *Invest Ophthalmol Vis Sci* 2008;49(5):2071–2076.
37. Kondo N, Honda S, Ishibashi K, Tsukahara Y, Negi A. LOC387715/HTRA1 variants in polypoidal choroidal vasculopathy and age-related macular degeneration in a Japanese population. *Am J Ophthalmol* 2007;144(4):608–612.
38. Magnusson KP, Duan S, Sigurdsson H, et al. *CFH* Y402H confers similar risk of soft drusen and both forms of late AMD. *PLoS Med* 2006;3(1):e5.
39. Fritsche LG, Loenhardt T, Janssen A, et al. Age-related macular degeneration is associated with an unstable ARMS2 (LOC387715) mRNA. *Nat Genet* 2008;40(7):892–896.
40. Deangelis MM, Ji F, Adams S, et al. Alleles in the HtrA serine peptidase 1 gene alter the risk of neovascular age-related macular degeneration. *Ophthalmology* 2008;115(7):1209–1215.e7.
41. Sakurada Y, Kubota T, Mabuchi F, Imasawa M, Tanabe N, Iijima H. Association of LOC387715 A69S with vitreous hemorrhage in polypoidal choroidal vasculopathy. *Am J Ophthalmol* 2008;145(6):1058–1062.
42. Lee KY, Vithana EN, Mathur R, et al. Association analysis of CFH, C2, BF, and HTRA1 gene polymorphisms in Chinese patients with polypoidal choroidal vasculopathy. *Invest Ophthalmol Vis Sci* 2008;49(6):2613–2619.
43. Gotoh N, Nakanishi H, Hayashi H, et al. ARMS2 (LOC387715) variants in Japanese patients with exudative age-related macular degeneration and polypoidal choroidal vasculopathy. *Am J Ophthalmol* 2009;147(6): 1037–1041.
44. Yanagisawa S, Kondo N, Miki A, et al. Difference between age-related macular degeneration and polypoidal choroidal vasculopathy in the hereditary contribution of the A69S variant of the age-related maculopathy susceptibility 2 gene (ARMS2). *Mol Vis* 2011;17:3574–3582.
45. Schmitz-Valckenberg S, Steinberg JS, Fleckenstein M, Visvalingam S, Brinkmann CK, Holtz FG. Combined confocal scanning laser ophthalmoscopy and spectral-domain optical coherence tomography imaging of reticular drusen associated with age-related macular degeneration. *Ophthalmology* 2010;117(6):1169–1176.
46. Sohrab MA, Smith RT, Salehi-Had H, Sadda SR, Fawzi AA. Image registration and multimodal imaging of reticular pseudodrusen. *Invest Ophthalmol Vis Sci* 2011;52(8):5743–5748.
47. Kertvely E, Hauck SM, Duetsch G, et al. ARMS2 is a constituent of the extracellular matrix providing a link between familial and sporadic age-related macular degenerations. *Invest Ophthalmol Vis Sci* 2010;51(1):79–88.

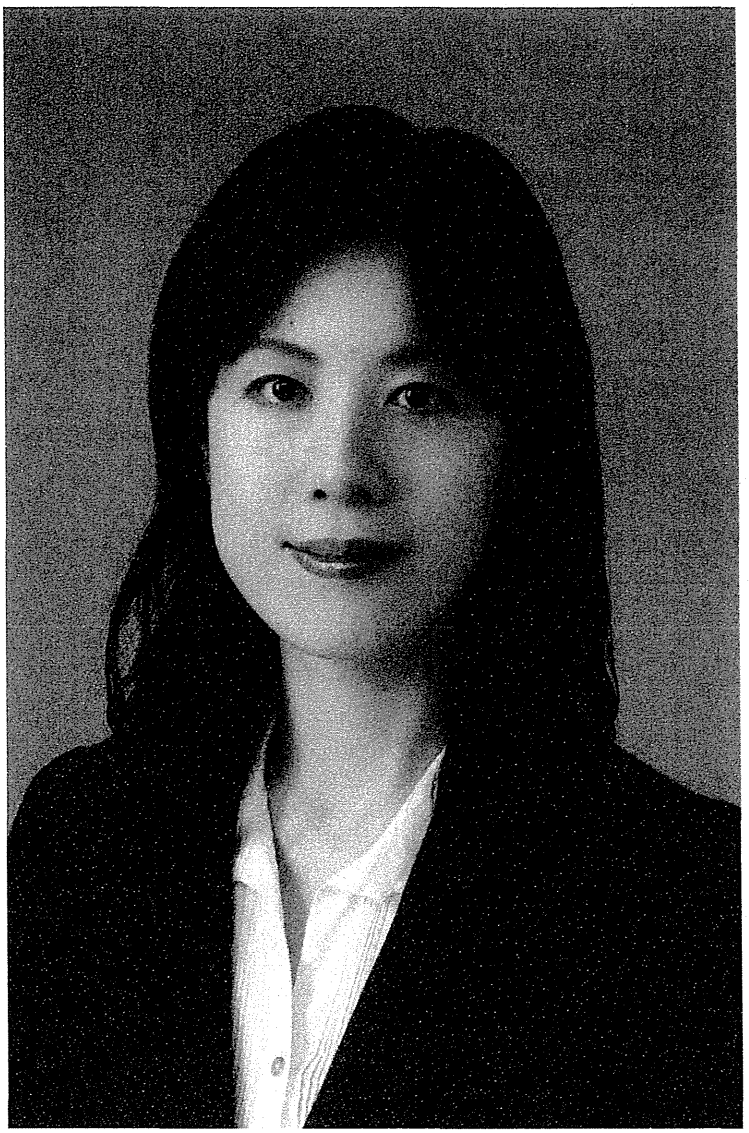

Biosketch

Naoko Ueda-Arakawa, MD, graduated from Kyoto University, Faculty of Medicine. She completed her residency program at Kyoto University Hospital and a fellowship at Osaka Red Cross Hospital, Osaka, Japan. She is now in a PhD program in the Department of Ophthalmology and Visual Sciences at Kyoto University under the supervisor of Professor Nagahisa Yoshimura. Her main interest is imaging analysis of macular diseases.

SUPPLEMENTAL TABLE. Prevalence of Reticular Pseudodrusen in Patients Over 70 Years of Age

	No. of Patients	No. of Patients With Reticular Pseudodrusen	Prevalence (%)
Typical AMD	67	8	11.9
PCV	53	2	3.8
RAP	11	10	90.9
Geographic atrophy	7	5	71.4
Combined[a]	8	3	37.5

AMD = age-related macular degeneration; PCV = polypoidal choroidal vasculopathy; RAP = retinal angiomatous proliferation.

[a]Patients with typical AMD, PCV, RAP, or geographic atrophy in 1 eye and another type of AMD in the other eye (4 typical AMD and PCV, 1 typical AMD and RAP, 1 typical AMD and geographic atrophy, 1 geographic atrophy and RAP, and 1 geographic atrophy and PCV).

Jpn J Ophthalmol (2012) 56:589–598
DOI 10.1007/s10384-012-0191-y

THE OFFICIAL INTERNATIONAL JOURNAL OF THE JAPANESE OPHTHALMOLOGICAL SOCIETY

CLINICAL INVESTIGATION

Visual prognosis of eyes with submacular hemorrhage associated with exudative age-related macular degeneration

Naoko Ueda-Arakawa · Akitaka Tsujikawa · Kenji Yamashiro · Sotaro Ooto · Hiroshi Tamura · Nagahisa Yoshimura

Received: 6 February 2012 / Accepted: 6 August 2012 / Published online: 4 October 2012

Abstract
Purpose To study the retinal structural changes associated with submacular hemorrhage due to exudative age-related macular degeneration (AMD) and their relationships with visual prognosis.
Methods We retrospectively reviewed the medical records of 31 consecutive patients (31 eyes) with visual impairment due to an acute submacular hemorrhage associated with typical AMD (10 eyes) or polypoidal choroidal vasculopathy (21 eyes).
Results Optical coherence tomography (OCT) revealed that submacular hemorrhage exhibited intense hyperreflectivity beneath the neurosensory retina and often seemed to infiltrate it. In the OCT sections, mild to moderate amorphous hyperreflectivity and/or hyperreflective dots were observed within the neurosensory retina, resulting in the loss of the junctions between the inner (IS) and outer (OS) segments of the photoreceptors. Of the 31 eyes, the foveal IS/OS line could be seen incompletely in 12 eyes and was totally absent in 16 eyes. The initial integrity of the foveal photoreceptor layer was correlated with the final visual acuity; the initial detection of the IS/OS just beneath the fovea was correlated with good final visual acuity ($r = 0.375$, $p = 0.038$).
Conclusion As a hallmark of integrity of the foveal photoreceptor layer, the initial detection of the IS/OS just beneath the fovea may predict good visual outcomes.

N. Ueda-Arakawa · A. Tsujikawa (✉) · K. Yamashiro · S. Ooto · H. Tamura · N. Yoshimura
Department of Ophthalmology and Visual Sciences, Kyoto University Graduate School of Medicine, 54 Shogoin-Kawahara-cho, Sakyo-ku, Kyoto 606-8507, Japan
e-mail: tujikawa@kuhp.kyoto-u.ac.jp

Keywords Age-related macular degeneration · Optical coherence tomography · Polypoidal choroidal vasculopathy · Submacular hemorrhage

Introduction

Submacular hemorrhage is a vision-threatening complication associated with exudative age-related macular degeneration (AMD) [1]. It can cause a sudden loss of central vision, often resulting in permanent visual loss [2]. The natural visual prognosis of submacular hemorrhage is extremely poor [3–6]. In a retrospective study by Bennett et al. [3], the mean initial visual acuity (VA) in eyes with submacular hemorrhage (20/860) improved to no better than 20/480 after a mean follow-up of three years. Numerous surgical procedures and several modifications are described, aimed at improving the poor visual prognosis [3–14]. For acute large submacular hemorrhage, surgical drainage or pneumatic displacement either with or without tissue plasminogen activator is thought to improve the visual prognosis [8, 11–14]. However, the effectiveness of subretinal clot removal is limited [7, 8].

The exact mechanism as to why a thick submacular hemorrhage can cause sudden visual loss remains unclear, even when the sensory retina within the macular area can be clearly seen on fundus examination [2]. Histologic reports show that submacular hemorrhage can cause substantial damage to the outer retina [16, 17]. In experimental studies with an animal model, Glatt and Machemer [18] report that the photoreceptors overlying areas of the hemorrhage appear to have degenerated and exhibit pyknosis within 24 h. Subsequent reports suggest other mechanisms of damage to the photoreceptor layer, including clot

retraction [19], iron toxicity [20, 21], and blockage of nutrient diffusion [2].

Optical coherence tomography (OCT) enables the detection of changes in the retinal architecture and quantitative measurement of retinal thickness [22–25]. Recent advances in OCT technology contributed to a more detailed understanding of the pathomorphology of many macular diseases [26–28]. However, there is still little information available on morphologic changes in the neurosensory retina associated with the submacular hemorrhage [15]. In addition, various factors are thought to be associated with visual prognosis in eyes with a submacular hemorrhage, including hemorrhage size [4, 6], elevation of the overlying retina [3, 4, 6], and the etiology of the original disease [3, 5]. However, quantitative evaluations are limited. In the present study, we studied OCT sections of eyes with submacular hemorrhage associated with exudative AMD. This was done to elucidate the structural changes in the overlying neurosensory retina in order to measure each characteristic manifestation quantitatively and to study the associations between the structural changes and visual function. Based on the results of these evaluations, we can now prognosticate the visual outcome of eyes with acute submacular hemorrhage.

Subjects and methods

For this observational case study, we retrospectively reviewed the medical records of 31 consecutive patients (31 eyes) with visual impairment due to an acute thick submacular hemorrhage associated with exudative AMD; each of these patients had visited the Macula Service of the Department of Ophthalmology at Kyoto University Hospital between April 2007 and March 2010. Of the 31 eyes, 10 had typical AMD and 21 had polypoidal choroidal vasculopathy (PCV). All 31 eyes included in this study exhibited a submacular hemorrhage just beneath the center of the fovea. Eyes with either a small subretinal hemorrhage with <1 disc area or an old yellowish discolored submacular hemorrhage were excluded. Each patient underwent angiography with a confocal laser scanning system (HRA-2, Heidelberg Engineering, Heidelberg, Germany). In the current study, the presence of choroidal neovascularization (CNV) was confirmed with fluorescein and indocyanine green angiography, which were performed either at the initial visit or after the resolution of the submacular hemorrhage. The diagnosis of PCV was based on indocyanine green angiography, which shows a branching vascular network that terminates in polypoidal swelling. Eyes with other macular abnormalities (e.g., pathologic myopia, idiopathic CNV, presumed ocular histoplasmosis, angioid streaks, other secondary CNV, or retinal arterial macroaneurysm) were excluded. Of the 31 eyes of our patients, 21 were treated with intravitreal injections of antivascular endothelial growth factor agents, 2 by photodynamic therapy, and 1 by pneumatic displacement of the submacular hemorrhage. This study was approved by the Institutional Review Board of the Kyoto University Graduate School of Medicine and adhered to the tenets of the Declaration of Helsinki.

At the initial examination after the submacular hemorrhage had occurred, each patient underwent a comprehensive ophthalmologic examination, including measurement of best-corrected VA, determination of intraocular pressure, indirect ophthalmoscopy, slit-lamp biomicroscopy with a non-contact lens, and examinations with the Spectralis HRA+OCT (Heidelberg Engineering). Using these initial OCT images, we measured the thickness of the neurosensory retina, the thickness of the submacular hemorrhage, and the total foveal thickness (Fig. 1). When the retinal pigment epithelium (RPE) was not visible under the fovea because of an overlying thick submacular hemorrhage, the OCT measurements were made from a presumed RPE line obtained from a clearly detectable RPE line in a more peripheral retinal area not covered by the hemorrhage. Furthermore, to assess the integrity of the outer foveal photoreceptor layer, we examined the junction between the inner and outer segments of the photoreceptor (IS/OS) line and the external limiting membrane (ELM) line in the fovea. The status of the IS/OS and ELM lines under the fovea was defined as complete, incomplete, or absent. To assess the density of the submacular hemorrhage, the detection of the underlying RPE line was also determined as complete, incomplete, or absent.

At the final examination, best-corrected VA was measured and indirect ophthalmoscopy, slit-lamp biomicroscopy with a noncontact lens, and examinations with the Spectralis HRA+OCT were performed, and all eyes showed complete resolution of the submacular hemorrhage beneath the fovea. After the submacular hemorrhage was resolved, the patients often exhibited a subfoveal mass, which appeared as a subretinal deposit or fibrosis on the fundus photographs. Since it was often difficult to determine its border with respect to the RPE, we performed three measurements in the fovea using the OCT images obtained at the final examination, including the thickness of the neurosensory retina, thickness of the subretinal mass and Bruch's membrane, and the total thickness (Fig. 1). The thickness of the neurosensory retina was defined as the distance between the vitreoretinal interface and the inner border of hyperreflectivity of either the RPE or the subretinal mass. The thickness of the subretinal mass and Bruch's membrane was defined as the distance between the outer border of the neurosensory retina and the fine straight line of the elastic fiber layer of the Bruch's membrane. Total thickness was defined as the distance between the

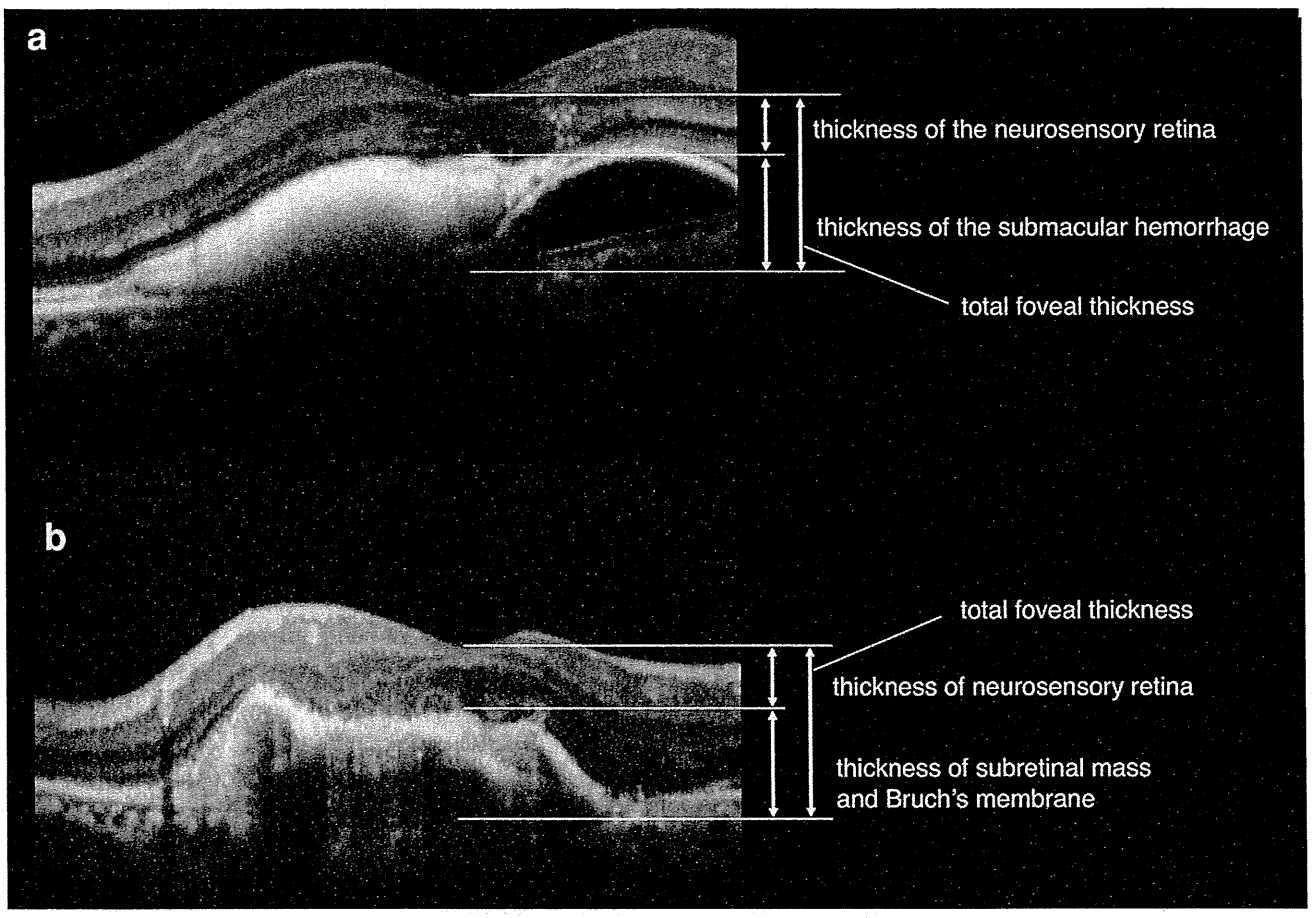

Fig. 1 **a** A cross-sectional image of the fovea obtained with optical coherence tomography (OCT) of an eye with acute submacular hemorrhage associated with exudative age-related macular degeneration. Using an acute OCT image, three measurements were made in the fovea, including the thickness of the neurosensory retina, thickness of the submacular hemorrhage, and total foveal thickness. **b** A cross-sectional image of the fovea obtained with OCT after resolution of the submacular hemorrhage. Using the final OCT image, three measurements were made in the fovea, including the thickness of the neurosensory retina, thickness of the subretinal mass and Bruch's membrane, and total foveal thickness

vitreoretinal interface and the elastic fiber layer of Bruch's membrane. These measurements and evaluations were performed by one retinal specialist.

All statistical analyses were performed using StatView version 4.5 (SAS Institute, Cary, NC, USA). All values are expressed as the mean ± standard deviation. For statistical analysis, VA measured using a Landolt chart was converted to the logarithm of the minimal angle of resolution (logMAR). In the current study, 1 optic disc area is equal to 2.54 mm^2 based on an optic disc diameter of 1.8 mm [29]. Bivariate relationships were analyzed using Pearson's correlation coefficient. P values <0.05 were considered statistically significant.

Results

In the current study, 31 eyes of 31 patients (21 men and 10 women; age range 66–93 years; mean age 76.8 ± 7.4 years) with submacular hemorrhage were examined. Of the 31 eyes, 21 had PCV and 10 had typical AMD. Table 1 shows the characteristics of the patients included in this study. The mean initial VA (logMAR) was 0.69 ± 0.45. The mean initial area and thickness of the submacular hemorrhage were 6.0 ± 3.1 disc areas and 315.0 ± 222.5 l m, respectively. The follow-up period was 11.3 ± 7.0 months, ranging from 3 to 28 months.

At the initial examination, each eye exhibited a submacular hemorrhage that affected the fovea. Upon OCT examination, the submacular hemorrhage exhibited intensive or moderate hyperreflectivity depending on its density beneath the neurosensory retina. Of the 31 eyes, the underlying RPE could not be seen at all in 8 because of the shadow cast by the submacular hemorrhage. In addition, the submacular hemorrhage from the CNV or polypoidal lesions seemed to infiltrate the overlying neurosensory retina in many cases. On OCT sections, mild to moderate amorphous hyperreflectivity and/or hyperreflective dots

Table 1 Initial and final conditions of patients with submacular hemorrhage associated with exudative age-related macular degeneration

Age (years)	76.8 ± 7.4
Gender (women/men)	10/21
Type of disease (typical AMD/PCV)	10/21
Initial examination	
Visual acuity (logMAR)	0.69 ± 0.45
Size of submacular hemorrhage (disc areas)	6.0 ± 3.1
Thickness of the neurosensory retina (l m)	194.3 ± 130.3
Thickness of the submacular hemorrhage (l m)	315.0 ± 222.5
Total foveal thickness (l m)	509.2 ± 281.0
Detection of IS/OS under the fovea (complete/incomplete/absent)	3/12/16
Detection of ELM under the fovea (complete/incomplete/absent)	21/2/8
Detection of RPE under the fovea (complete/incomplete/absent)	8/15/8
Duration of symptom (months)	3.7 ± 2.3
Follow-up (months)	11.3 ± 7.0
Final examination	
Visual acuity (logMAR)	0.69 ± 0.47
Cystoid macular edema (%)	11 (35.5 %)
Subfoveal mass (%)	20 (64.5 %)
Thickness of neurosensory retina (l m)	175.4 ± 136.3
Subretinal deposit and Bruch's membrane (l m)	169.5 ± 150.4
Total foveal thickness (l m)	363.7 ± 203.8
Detection of IS/OS under the fovea (complete/incomplete/absent)	3/8/20
Detection of ELM under the fovea (complete/incomplete/absent)	16/5/10

AMD age-related macular degeneration, *PCV* polypoidal choroidal vasculopathy, *logMAR* logarithm of the minimum angle of resolution, *IS/OS* junction between the inner and outer segments of the photoreceptors, *ELM* external limiting membrane, *RPE* retinal pigment epithelium

were seen in the overlying neurosensory retina, especially in the outer aspect, resulting in a lack of IS/OS or ELM lines (Fig. 2). Of the 31 eyes, the foveal IS/OS line could not be observed completely in 28, whereas the foveal ELM line could be observed completely in 21. Intraretinal hyperreflective lesions due to submacular hemorrhage were occasionally observed mainly outside the ELM. In these eyes, the ELM seemed to work as a blocking agent against the hemorrhage (Fig. 2).

Table 2 shows the relationships between the initial VA and other measured values obtained at the initial examination. The etiology of the original disease (typical AMD or PCV) was not correlated with the initial VA ($r = 0.194$, $p = 0.300$). However, the size and thickness of the submacular hemorrhage were both correlated with the initial VA ($r = 0.411$, $p = 0.022$; $r = 0.485$, $p = 0.0057$). In addition, detection of the RPE beneath the fovea, which seemed to reflect the density of the submacular hemorrhage, was correlated with the initial VA ($r = 0.479$, $p = 0.0064$). While the thickness of the neurosensory retina was not correlated with the initial VA ($r = 0.203$, $p = 0.274$), detection of the foveal ELM was correlated with initial VA ($r = 0.423$, $p = 0.018$).

At the final examination, all eyes exhibited a complete absorption of the submacular hemorrhage, and the mean final VA was 0.69 ± 0.47 (logMAR). Cystoid macular edema was observed in 11 eyes. Twenty eyes exhibited a subretinal mass, the mean thickness of which, including the Bruch's membrane, was 169.5 ± 150.4 l m. In addition, submacular hemorrhages caused substantial damage to the overlying outer retina. The IS/OS were completely detected in only 3 and the ELM lines in 16 eyes.

Table 3 shows the relationships between the final VA and other measured values obtained at the final examination. The etiology of the original disease (typical AMD or PCV) was not correlated with the final VA ($r = 0.249$, $p = 0.176$). However, cystoid macular edema and subfoveal mass were correlated with poor final VA ($r = 0.355$, $p = 0.050$; $r = 0.477$, $p = 0.0067$). The total retinal thickness and the thickness of the subfoveal mass at the final examination were correlated with poor final VA ($r = 0.607$, $p = 0.0003$; $r = 0.489$, $p = 0.0052$). In addition, the integrity of the foveal photoreceptor layer contributed to foveal function. Detection of the IS/OS and ELM lines beneath the fovea were both strongly correlated with good final VA ($r = 0.574$, $p = 0.0007$; $r = 0.756$, $p < 0.0001$).

Table 4 shows the relationships between the final VA and measured values obtained at the initial examination. The final VA was 0.86 ± 0.39 with typical AMD and 0.61 ± 0.49 with PCV ($p = 0.176$). The etiology of the original disease was not correlated with the final VA ($r = 0.249$, $p = 0.176$). Although the submacular hemorrhage thickness and density were weakly correlated with the

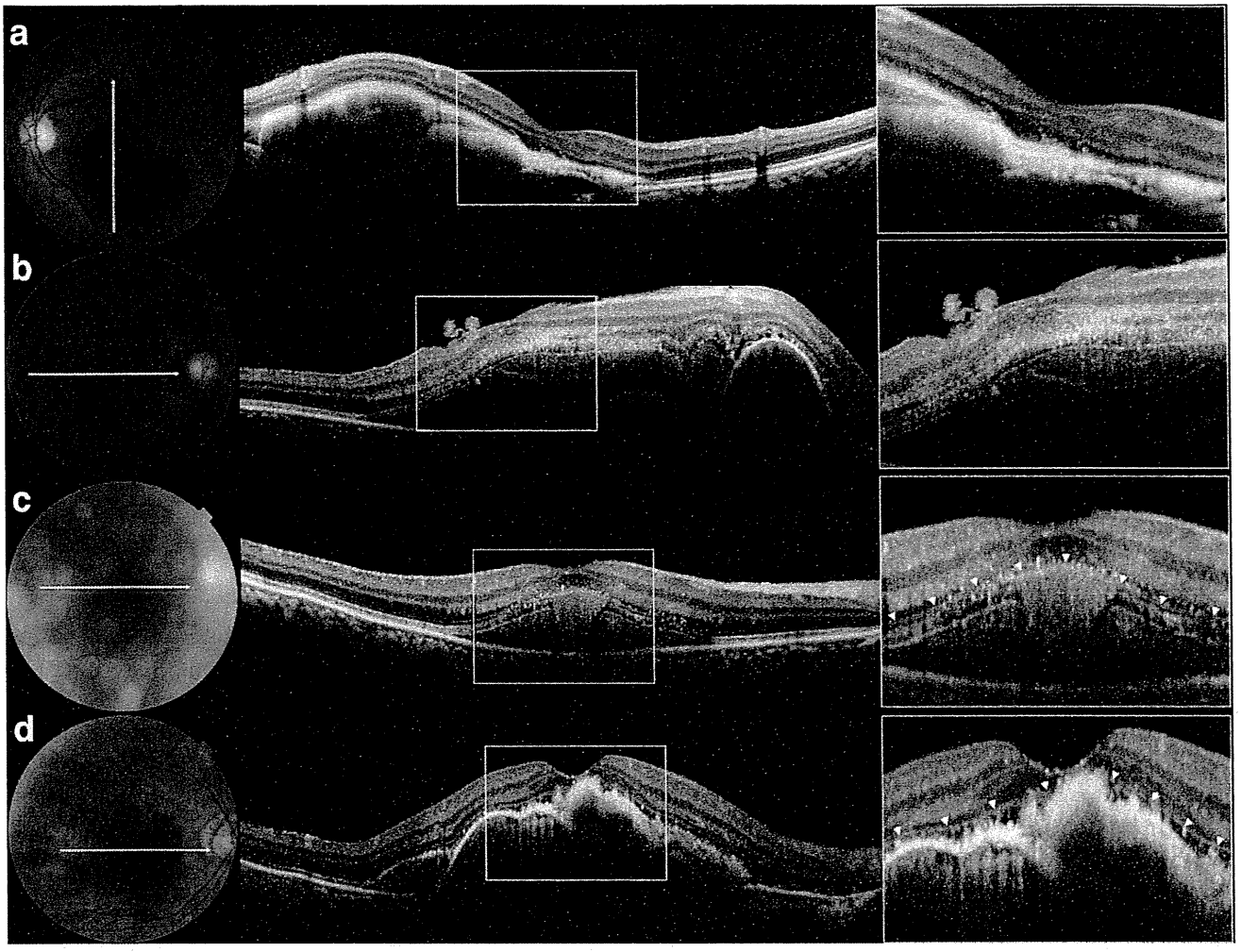

Fig. 2 Cross-sectional images obtained by optical coherence tomography (OCT) in eyes with acute submacular hemorrhage associated with exudative age-related macular degeneration. Each OCT section (*middle* in each case) was made along an *arrow* shown in the fundus photographs (*left* in each case). Magnified OCT images (*right* in each case) were made from the delimited boxes in OCT sections. **a** On the OCT section, the submacular hemorrhage shows intensive hyperreflectivity beneath the neurosensory retina. Within the outer aspect of the neurosensory retina, several *hyperreflective dots* are seen. The structure of the neurosensory retina seems to be relatively well preserved. Visual acuity was 0.5. **b** On the OCT section, submacular hemorrhage shows moderate hyperreflectivity. Amorphous hyperreflectivity and numerous hyperreflective dots are seen within the neurosensory retina. Visual acuity was 0.09. **c** On the OCT section, submacular hemorrhage shows moderate hyperreflectivity. Amorphous hyperreflectivity and numerous hyperreflective dots are seen in neurosensory retina, especially in the outer aspect. Under the fovea, infiltration of the hemorrhage into the neurosensory retina seems to be blocked by the external limiting membrane (*arrowheads*). Visual acuity was 0.4. **d** On the OCT section, submacular hemorrhage shows intensive hyperreflectivity. Under the fovea, the hemorrhage seems to invade the neurosensory retina beyond the external limiting membrane (*arrowheads*). Visual acuity was 0.08

final VA ($r = 0.258$, $p = 0.161$; $r = 0.281$, $p = 0.126$), the size of the submacular hemorrhage was not ($r = 0.111$, $p = 0.554$). However, the initial integrity of the foveal photoreceptor layer was correlated with visual prognosis. While the initial detection of the ELM beneath the fovea was not correlated with final VA ($r = 0.063$, $p = 0.736$), the initial detection of the IS/OS beneath the fovea was correlated with good final VA ($r = 0.375$, $p = 0.038$) (Figs. 3, 4). In the subgroup analysis, eyes with typical AMD and PCV exhibited a similar tendency, respectively, although the correlations were not statistically significant ($r = 0.566$, $p = 0.088$ with AMD; $r = 0.331$, $p = 0.142$ with PCV); this is possibly due to the small number of eyes in each group.

Discussion

Acute serous retinal detachment associated with central serous chorioretinopathy does not usually cause a severe decrease in VA, even if there is subretinal fluid under the fovea [30]. However, submacular hemorrhage often

Table 2 Association of initial visual acuity with other measurements obtained at the initial examination

	r	*p* value
Age (years)	0.018	0.922
Type of disease (typical AMD/PCV)	0.194	0.300
Size of submacular hemorrhage (disc areas)	0.411	0.022
Thickness of the neurosensory retina (l m)	0.203	0.274
Thickness of the submacular hemorrhage (l m)	0.485	0.0057
Total foveal thickness (l m)	0.478	0.0065
Detection of IS/OS under the fovea	0.272	0.139
Detection of ELM under the fovea	0.423	0.018
Detection of RPE under the fovea	0.479	0.0064

AMD age-related macular degeneration, *PCV* polypoidal choroidal vasculopathy, *logMAR* logarithm of the minimum angle of resolution, *IS/OS* junction between the inner and outer segments of the photoreceptors, *ELM* external limiting membrane, *RPE* retinal pigment epithelium

Table 3 Association of final visual acuity with other measurements obtained at the final examination

	r	*p* value
Age (years)	0.244	0.186
Type of disease (typical AMD/PCV)	0.249	0.176
Duration of symptom (months)	0.182	0.327
Cystoid macular edema	0.355	0.050
Subfoveal mass	0.477	0.0067
Thickness of the neurosensory retina (l m)	0.277	0.132
Thickness of subretinal mass and Bruch's membrane (l m)	0.489	0.0052
Total foveal thickness (l m)	0.607	0.0003
Detection of IS/OS under the fovea (%)	0.574	0.0007
Detection of ELM under the fovea (%)	0.756	<0.0001

AMD age-related macular degeneration, *PCV* polypoidal choroidal vasculopathy, *logMAR* logarithm of the minimum angle of resolution, *RPE* retinal pigment epithelium, *IS/OS* the junction between inner and outer segments of the photoreceptors, *ELM* external limiting membrane

Table 4 Association of final visual acuity with measurements obtained at the initial examination

	r	*p* value
Age (years)	0.244	0.186
Type of disease (typical AMD/PCV)	0.249	0.176
Size of subretinal hemorrhage (disc areas)	0.111	0.554
Visual acuity (logMAR)	0.295	0.107
Thickness of the neurosensory retina (l m)	0.100	0.594
Thickness of the submacular hemorrhage (l m)	0.268	0.145
Total foveal thickness (l m)	0.258	0.161
Detection of IS/OS under the fovea	0.375	0.038
Detection of ELM under the fovea	0.063	0.736
Detection of RPE under the fovea	0.281	0.126

AMD age-related macular degeneration, *PCV* polypoidal choroidal vasculopathy, *logMAR* logarithm of the minimum angle of resolution, *IS/OS* junction between the inner and outer segments of the photoreceptors, *ELM* external limiting membrane, *RPE* retinal pigment epithelium

accompanies acute severe visual loss immediately after onset [2]. Histologic reports show that submacular hemorrhage causes severe damage to the outer retina [16, 17], and experimental reports suggest mechanisms by which chronic damage to the photoreceptor layer occurs [18, 19]. However, in addition to chronic effects, bleeding within the subretinal space can exert immediate effects on the neurosensory retina, thereby causing acute visual dysfunction [15].

The initial OCT sections of our patients revealed that the submacular hemorrhage exhibited hyperreflectivity beneath the neurosensory retina. In addition, the overlying neurosensory retina often exhibited hyperreflective lesions. In the current study, amorphous hyperreflectivity of various intensities and hyperreflective dots were observed in the outer aspect of the overlying neurosensory retina. Immediately after bleeding within the subretinal space, erythrocytes, macrophages, and fibrin can migrate into the outer retina and may destroy the integrity of the photoreceptor layer [31]. Ooto et al. [32] report the relationship between VA and fibrin infiltration within the neurosensory retina in eyes with PCV. In addition, Coscas et al. [27] state that bright hyperreflective spots and hyperreflective material within the neurosensory retina could be derived from an inflammatory reaction, and they indicate the activity of exudative AMD. Based on previous reports [32, 33], our findings related to the neurosensory retina may be associated with acute dysfunction of the macula, which results in an acute loss of central vision.

In the current study, while the IS/OS line beneath the fovea was detected completely at the initial visit in only 3 eyes, complete detection of the ELM line under the fovea was achieved in 21 eyes. In fact, the ELM line was frequently preserved even in the eyes with a thick submacular hemorrhage. On OCT sections, the ELM line sometimes appeared to act as a blocking agent against the advancement of hemorrhage into the retina after the hemorrhage had already infiltrated the inner and outer segments. Our OCT findings can be explained according to the theory on the mechanisms of fluid movement proposed by Marmor [34]. He reports that the ELM, which consists of the zonula adherens between Müller cells and photoreceptors at the base of the outer segments, works as a weak anatomic barrier to the movement of large protein molecules in the retina.

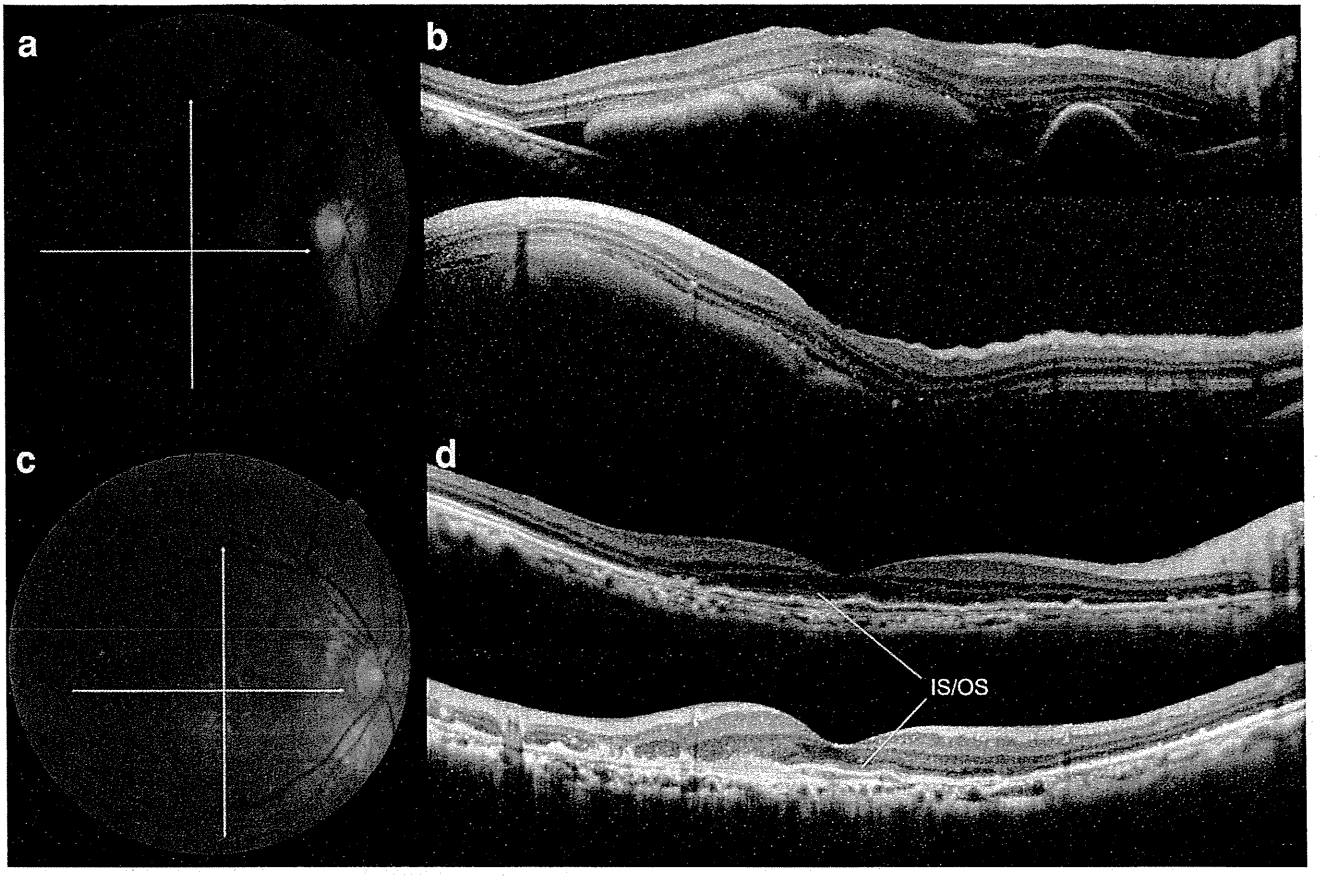

Fig. 3 Good recovery of vision in eyes with submacular hemorrhage associated with polypoidal choroidal vasculopathy. **a** A 66-year-old woman with a sudden decrease of vision in the right eye (0.2 OD), at which time she had a large submacular hemorrhage. **b** Initial horizontal (*upper*) and vertical (*lower*) optical coherence tomographic images along the *white arrows* shown in the fundus photograph show intensive hyperreflectivity of the submacular hemorrhage beneath the neurosensory retina. Several *hyperreflective dots* are seen in the neurosensory retina; but the structure of the neurosensory retina seems to be well preserved. The line of the junction between inner and outer segments of the photoreceptors (IS/OS) is seen under the fovea. **c** At 12 months, the submacular hemorrhage was completely absorbed. **d** Horizontal (*upper*) and vertical (*lower*) optical coherence tomographic images along the *white arrows* show good preservation of the neurosensory retina. The IS/OS line is seen under the fovea and visual acuity has improved to 0.8 OD

Previous reports on the natural history of submacular hemorrhage suggest that exudative AMD is associated with poor visual prognosis, especially when subretinal fibrosis is observed after the resolution of the hemorrhage [3, 5]. In the current study, 64.5 % of the eyes exhibited a subfoveal mass at the final examination; the thickness of this mass was strongly correlated with the final VA. In addition, recent studies with OCT show that the integrity of the foveal photoreceptor layer—especially its outer aspect—is necessary if good visual function is to be achieved [35]. A few years ago, Hayashi et al. [36] reported the association between intact foveal IS/OS and good VA after the successful treatment of exudative AMD with photodynamic therapy. Oishi et al. [37] suggest that foveal ELM is associated with final VA in exudative AMD treated with photodynamic therapy. Consistent with these reports, our study shows that after complete resolution of the submacular hemorrhage, complete detection of the IS/OS and ELM lines are correlated with final VA.

So far, various factors have been suggested to be associated with visual prognosis, including the initial VA [4, 5], size or thickness of the submacular hemorrhage [3, 4, 6], and etiology of the original disease [3, 5]. As mentioned above, visual prognosis was poor in the eyes with submacular hemorrhage resulting from exudative AMD [3], especially in the eyes with subretinal CNV [5]. While the relationship between the size of the hemorrhage and the final VA varies, most previous studies indicate that the initial thickness of the hemorrhage is associated with visual prognosis [3, 4, 6]. However, in those studies, the thickness of the submacular hemorrhage was evaluated as the elevation of the neurosensory retina detected by stereoscopic photography; no quantitative evaluations were performed. In the current study, the initial size of the hemorrhage was

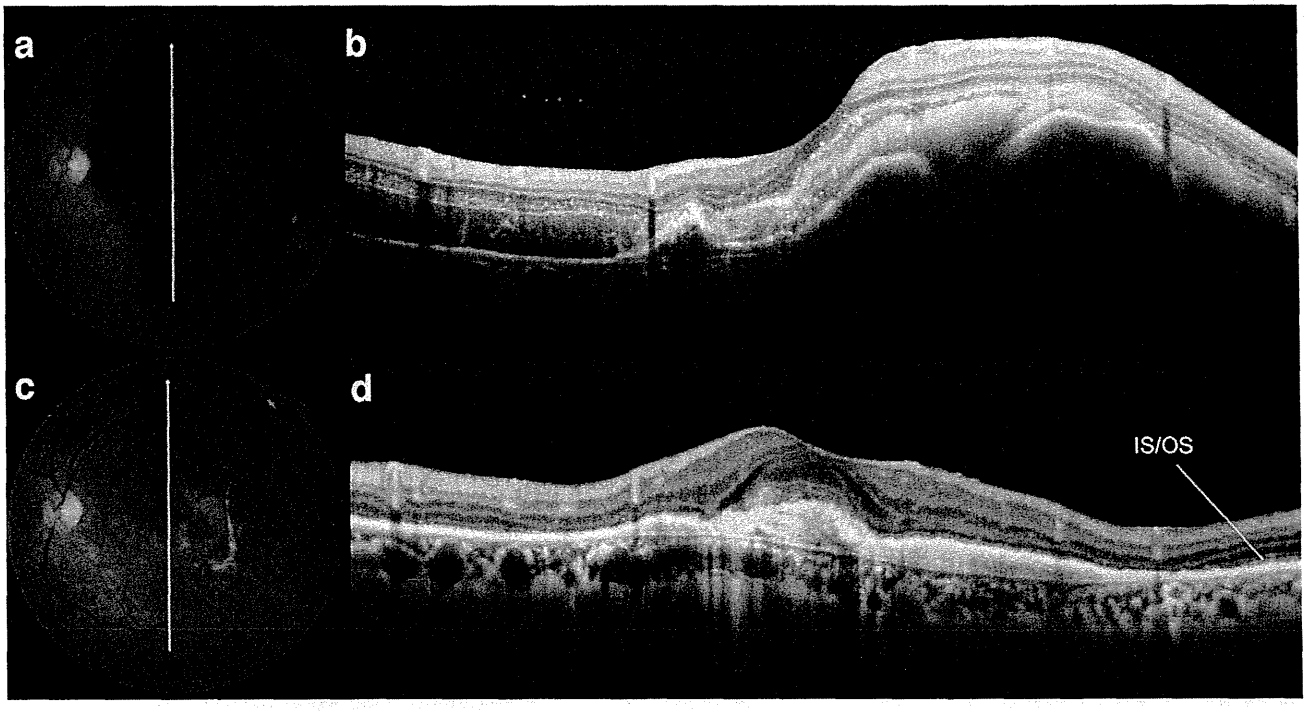

Fig. 4 Poor recovery of vision in eyes with submacular hemorrhage associated with polypoidal choroidal vasculopathy. **a** A 67-year-old man with a sudden decrease of vision in the left eye (0.4 OS), at which time he was noted to have a massive submacular hemorrhage. **b** Initial optical coherence tomographic image along the *white arrows* shown in the fundus photograph reveals intensive hyperreflectivity of the submacular hemorrhage beneath the neurosensory retina. Amorphous *hyperreflectivity and hyperreflective dots* are seen in overlying neurosensory retina. The line of the junction between inner and outer segments of the photoreceptors (IS/OS) is not detectable under the fovea. **c** At 14 months, the submacular hemorrhage has been absorbed completely. **d** Optical coherence tomographic image along the *white arrows* shows a thick subfoveal deposit. The IS/OS line is seen under the fovea, but visual acuity remained 0.3 OS

not correlated with the final VA. However, the thickness and density of the hemorrhage were both weakly correlated with final VA.

It is certain that the integrity of the outer photoreceptor layer in the fovea contributes to VA [35–38]. In the current study, initial detection of the ELM line beneath the fovea was correlated with the initial but not final VA. While the foveal ELM was initially detected in 21 eyes, complete detection was achieved at the final examination in only 16 eyes. The chronic harmful effects of submacular hemorrhage include damage to the foveal photoreceptor layer, which results in a decline in VA [16]. However, the initial detection of the foveal IS/OS line was correlated with visual prognosis. The inner and outer segments of the photoreceptor layer located outside the ELM, which are assumed to function as a blockade against hemorrhage infiltration [34], are vulnerable to acute submacular hemorrhage [19, 39]. The foveal IS/OS line was detected completely at the initial visit in only three of our patients. In such eyes, acute effects on the neurosensory retina may be minimal, resulting in good visual prognosis.

In experimental studies with animal models, the suggested mechanisms of damage to the photoreceptor layer include clot retraction [19], iron toxicity [20, 21], and blockage of nutrient diffusion by iron [18]. Submacular hemorrhage may block the exchange of nutrients and metabolites between the neurosensory retina and RPE [18]. The chief toxic agent released from submacular hemorrhage is thought to be iron in the form of ferritin [2]. In an experimental model of submacular hemorrhage, increased iron levels in the outer segments of the photoreceptor layer are thought to exert a toxic effect on the outer segment lipids via oxidative stress [39]. In addition, an experimental study by Toth et al. [19] shows that fibrin produced by submacular hemorrhage interdigitates with the outer photoreceptor segments and subsequently tears the sheet of both the inner and the outer photoreceptor segments. In the current study, the detection of the foveal IS/OS line at the initial examination was correlated with good final VA. In these eyes, the lack of fibrin interdigitation and the low level of iron toxicity could explain the good visual prognosis.

The limitations of the current study include its retrospective nature, various treatment regimens used, and small sample size. Treatment modality may have some influence on the visual prognosis [40, 41]. Several factors may be mutually related, but the number of eyes was too small to

perform multiple univariate testing. In addition, while no eyes showed residual submacular hemorrhage at the final visits, the follow-up period of some eyes was too short to discuss the visual prognosis [42]. Another limitation is that the current study involved eyes with typical AMD and PCV. However, despite these limitations, our findings suggest that submacular hemorrhages often infiltrate the overlying neurosensory retina, harming the structure of the outer retina. As a hallmark of the integrity of the foveal photoreceptor layer, the initial detection of the IS/OS just beneath the fovea may be associated with good visual outcomes. Previous studies report a better visual prognosis for PCV [43]. We analyzed the subgroups of typical AMD and PCV to confirm the correlation between the initial detection of the foveal IS/OS and final VA. Each group exhibited a similar tendency, but the correlation was not statistically significant, possibly because of the small number of eyes in each group. Further prospective studies are necessary to confirm the correlations reported in the current study.

References

1. Woo JJ, Lou PL, Ryan EA, Kroll AJ. Surgical treatment of submacular hemorrhage in age-related macular degeneration. Int Ophthalmol Clin. 2004;44:43–50.
2. Steel DH, Sandhu SS. Submacular haemorrhages associated with neovascular age-related macular degeneration. Br J Ophthalmol. 2011;95:1051–7.
3. Bennett SR, Folk JC, Blodi CF, Klugman M. Factors prognostic of visual outcome in patients with subretinal hemorrhage. Am J Ophthalmol. 1990;109:33–7.
4. Avery RL, Fekrat S, Hawkins BS, Bressler NM. Natural history of subfoveal subretinal hemorrhage in age-related macular degeneration. Retina. 1996;16:183–9.
5. Berrocal MH, Lewis ML, Flynn HW Jr. Variations in the clinical course of submacular hemorrhage. Am J Ophthalmol. 1996;122: 486–93.
6. Scupola A, Coscas G, Soubrane G, Balestrazzi E. Natural history of macular subretinal hemorrhage in age-related macular degeneration. Ophthalmologica. 1999;213:97–102.
7. de Juan E, Jr Machemer R. Vitreous surgery for hemorrhagic and fibrous complications of age-related macular degeneration. Am J Ophthalmol. 1988;105:25–9.
8. Wade EC, Flynn HW Jr, Olsen KR, Blumenkranz MS, Nicholson DH. Subretinal hemorrhage management by pars plana vitrectomy and internal drainage. Arch Ophthalmol. 1990;108:973–8.
9. Stifter E, Michels S, Prager F, Georgopoulos M, Polak K, Hirn C, et al. Intravitreal bevacizumab therapy for neovascular age-related macular degeneration with large submacular hemorrhage. Am J Ophthalmol. 2007;144:886–92.
10. Fine HF, Iranmanesh R, Del Priore LV, Barile GR, Chang LK, Chang S, et al. Surgical outcomes after massive subretinal hemorrhage secondary to age-related macular degeneration. Retina. 2010;30:1588–94.
11. Ohji M, Saito Y, Hayashi A, Lewis JM, Tano Y. Pneumatic displacement of subretinal hemorrhage without tissue plasminogen activator. Arch Ophthalmol. 1998;116:1326–32.
12. Kamei M, Tano Y, Maeno T, Ikuno Y, Mitsuda H, Yuasa T. Surgical removal of submacular hemorrhage using tissue plasminogen activator and perfluorocarbon liquid. Am J Ophthalmol. 1996;121:267–75.
13. Lim JI, Drews-Botsch C, Sternberg P Jr, Capone A Jr, Aaberg TM Sr. Submacular hemorrhage removal. Ophthalmology. 1995;102:1393–9.
14. Hassan AS, Johnson MW, Schneiderman TE, Regillo CD, Tornambe PE, Poliner LS, et al. Management of submacular hemorrhage with intravitreous tissue plasminogen activator injection and pneumatic displacement. Ophthalmology. 1999;106:1900–6.
15. Tsujikawa A, Sakamoto A, Ota M, Oh H, Miyamoto K, Kita M, et al. Retinal structural changes associated with retinal arterial macroaneurysm examined with optical coherence tomography. Retina. 2009;29:782–92.
16. Green WR, Key SN 3rd. Senile macular degeneration: a histopathologic study. Trans Am Ophthalmol Soc. 1977;75:180–254.
17. Reynders S, Lafaut BA, Aisenbrey S, Broecke CV, Lucke K, Walter P, et al. Clinicopathologic correlation in hemorrhagic age-related macular degeneration. Graefes Arch Clin Exp Ophthalmol. 2002;240:279–85.
18. Glatt H, Machemer R. Experimental subretinal hemorrhage in rabbits. Am J Ophthalmol. 1982;94:762–73.
19. Toth CA, Morse LS, Hjelmeland LM, Landers MB 3rd. Fibrin directs early retinal damage after experimental subretinal hemorrhage. Arch Ophthalmol. 1991;109:723–9.
20. Koshibu A. Ultrastructural studies on absorption of an experimentally produced subretinal hemorrhage. III. Absorption of erythrocyte break down products and retinal hemosiderosis at the late stage. Nippon Ganka Gakkai Zasshi. 1979;83:386–400. (in Japanese).
21. el Baba F, Jarrett WH 2nd, Harbin TS Jr, Fine SL, Michels RG, Schachat AP, et al. Massive hemorrhage complicating age-related macular degeneration. Clinicopathologic correlation and role of anticoagulants. Ophthalmology. 1986;93:1581–92.
22. Drexler W, Sattmann H, Hermann B, Ko TH, Stur M, Unterhuber A, et al. Enhanced visualization of macular pathology with the use of ultrahigh-resolution optical coherence tomography. Arch Ophthalmol. 2003;121:695–706.
23. Ko TH, Fujimoto JG, Schuman JS, Paunescu LA, Kowalevicz AM, Hartl I, et al. Comparison of ultrahigh- and standard-resolution optical coherence tomography for imaging macular pathology. Ophthalmology. 2005;112:1922–35.
24. Wojtkowski M, Bajraszewski T, Gorczynska I, Targowski P, Kowalczyk A, Wasilewski W, et al. Ophthalmic imaging by spectral optical coherence tomography. Am J Ophthalmol. 2004; 138:412–9.
25. Chen TC, Cense B, Pierce MC, Nassif N, Park BH, Yun SH, et al. Spectral domain optical coherence tomography: ultra-high speed, ultra-high resolution ophthalmic imaging. Arch Ophthalmol. 2005;123:1715–20.
26. Coscas F, Coscas G, Souied E, Tick S, Soubrane G. Optical coherence tomography identification of occult choroidal neovascularization in age-related macular degeneration. Am J Ophthalmol. 2007;144:592–9.
27. Coscas G, Coscas F, Vismara S, Zourdani A, Li Calzi CI. Clinical features and natural history of AMD. In: Coscas G, Coscas F, Vismara S, Zourdani A, Li Calzi CI, editors. Optical coherence tomography in age-related macular degeneration. Heidelberg: Springer, 2009. p. 171–274.
28. Mavrofrides EC, Villate N, Rosenfeld PJ, Puliafito CA. Age-related macular degeneration. 2nd ed. In: Schuman JS, Puliafito CA, Fujimoto JG, editors. Optical coherence tomography. Thorofare: Slack; 2004. p. 243–344.
29. Rosenfeld PJ, Brown DM, Heier JS, Boyer DS, Kaiser PK, Chung CY, et al. Ranibizumab for neovascular age-related macular degeneration. N Engl J Med. 2006;355:1419–31.

30. Spaide RF. Central serous chorioretinopathy. In: Holz FG, Spaide RF, editors. Medical retina. Berlin: Springer; 2004. p. 77–93.
31. Lincoff H, Madjarov B, Lincoff N, Movshovich A, Saxena S, Coleman DJ, et al. Pathogenesis of the vitreous cloud emanating from subretinal hemorrhage. Arch Ophthalmol. 2003;121:91–6.
32. Ooto S, Tsujikawa A, Mori S, Tamura H, Yamashiro K, Otani A, et al. Retinal microstructural abnormalities in central serous chorioretinopathy and polypoidal choroidal vasculopathy. Retina. 2011;31:527–34.
33. Coscas G, Coscas F, Vismara S, Zourdani A, Li Calzi CI. OCT interpretation. In: Coscas G, Coscas F, Vismara S, Zourdani A, Li Calzi CI, editors. Optical coherence tomography in age-related macular degeneration. Heidelberg: Springer; 2009. p. 97–170.
34. Marmor MF. Mechanisms of fluid accumulation in retinal edema. Doc Ophthalmol. 1999;97:239–49.
35. Costa RA, Calucci D, Skaf M, Cardillo JA, Castro JC, Melo LA Jr, et al. Optical coherence tomography 3: automatic delineation of the outer neural retinal boundary and its influence on retinal thickness measurements. Invest Ophthalmol Vis Sci. 2004;45: 2399–406.
36. Hayashi H, Yamashiro K, Tsujikawa A, Ota M, Otani A, Yoshimura N. Association between foveal photoreceptor integrity and visual outcome in neovascular age-related macular degeneration. Am J Ophthalmol. 2009;148:83–9.
37. Oishi A, Hata M, Shimozono M, Mandai M, Nishida A, Kurimoto Y. The significance of external limiting membrane status for visual acuity in age-related macular degeneration. Am J Ophthalmol. 2010;150:27–32.
38. Sandberg MA, Brockhurst RJ, Gaudio AR, Berson EL. The association between visual acuity and central retinal thickness in retinitis pigmentosa. Invest Ophthalmol Vis Sci. 2005;46:3349–54.
39. Bhisitkul RB, Winn BJ, Lee OT, Wong J, Pereira Dde S, Porco TC, et al. Neuroprotective effect of intravitreal triamcinolone acetonide against photoreceptor apoptosis in a rabbit model of subretinal hemorrhage. Invest Ophthalmol Vis Sci. 2008;49: 4071–7.
40. Kim KS, Lee WK. Bevacizumab for serous changes originating from a persistent branching vascular network following photodynamic therapy for polypoidal choroidal vasculopathy. Jpn J Ophthalmol. 2011;55:370–7.
41. Nakata I, Yamashiro K, Nakanishi H, Tsujikawa A, Otani A, Yoshimura N. VEGF gene polymorphism and response to intravitreal bevacizumab and triple therapy in age-related macular degeneration. Jpn J Ophthalmol. 2011;55:435–43.
42. Akaza E, Yuzawa M, Mori R. Three-year follow-up results of photodynamic therapy for polypoidal choroidal vasculopathy. Jpn J Ophthalmol. 2011;55:39–44.
43. Sho K, Takahashi K, Yamada H, Wada M, Nagai Y, Otsuji T, et al. Polypoidal choroidal vasculopathy: incidence, demographic features, and clinical characteristics. Arch Ophthalmol. 2003;121: 1392–6.

Molecular Vision 2012; 18:2726-2735 <http://www.molvis.org/molvis/v18/a280>
Received 6 June 2012 | Accepted 15 November 2012 | Published 17 November 2012

Association of *paired box 6* with high myopia in Japanese

Masahiro Miyake,[1,2] Kenji Yamashiro,[1] Hideo Nakanishi,[1,2] Isao Nakata,[1,2] Yumiko Akagi-Kurashige,[1,2] Akitaka Tsujikawa,[1] Muka Moriyama,[3] Kyoko Ohno-Matsui,[3] Manabu Mochizuki,[3] Ryo Yamada,[2] Fumihiko Matsuda,[2] Nagahisa Yoshimura[1]

[1]Department of Ophthalmology and Visual Sciences, Kyoto University Graduate School of Medicine, Kyoto, Japan; [2]Center for Genomic Medicine, Kyoto University Graduate School of Medicine, Kyoto, Japan; [3]Department of Ophthalmology and Visual Science, Tokyo Medical and Dental University, Tokyo, Japan

Purpose: The objective of this study was to investigate whether genetic variations in the *paired box 6* (*PAX6*) gene are associated with high myopia in Japanese subjects.

Methods: A total of 1,307 unrelated Japanese patients with high myopia (axial length ≥26 mm in both eyes) and two independent control groups were evaluated (333 cataract patients without high myopia and 923 age-matched healthy Japanese individuals). We genotyped three tag single-nucleotide polymorphisms (SNPs) in *PAX6*: rs2071754, rs644242, and rs3026354. These SNPs provided 100% coverage of all phase II HapMap SNPs within the *PAX6* region (minor allele frequency ≥0.10; r^2 threshold: 0.90). Chi-square tests for trend and multivariable logistic regression were conducted.

Results: Genotype distributions in the three SNPs were in accordance with the Hardy–Weinberg equilibrium. After adjusting for age and sex, evaluation of cataract control showed a marginal association with high myopia in rs644242 (odds ratio [95% confidence interval]=0.69 [0.49–0.96], p=0.026), and a significant association was observed in healthy Japanese controls (0.79 [0.66–0.96], p=0.015). We pooled two control cohorts to evaluate the association. This analysis revealed a strong association between rs644242 and high myopia (0.78 [0.65–0.92], p=0.0045). The rs644242 A allele was a protective allele for development of high myopia. Subanalysis also revealed that rs644242 was significantly associated with extreme high myopia (0.78 [0.64–0.95], p=0.0165). The other two SNPs did not show a significant association with this condition.

Conclusions: The current study showed a significant association of *PAX6* with high and extreme myopia in Japanese participants. The A allele of rs644242 is a protective allele.

Myopia is the most common visual disorder in the world and presents major public health concerns, especially in East Asian populations. Eyes with long axial lengths (≥26 mm) or a high degree of myopic refractive error (≤−6 diopter [D]) were diagnosed with high myopia [1]. High myopia is associated with various ocular complications [2], and pathological myopia is one of the leading causes of legal blindness in developed countries [3-5]. Therefore, clarifying the pathological pathway that leads to high myopia and developing methods for preventing or delaying its onset are important.

Myopia is a complex disease caused by environmental and genetic factors. Although linkage analysis studies have revealed more than 20 myopia-susceptibility loci and various candidate genes have been evaluated, most of these genes were not consistently responsible for high myopia. Recently, several groups performed genome-wide association studies (GWAS); we determined a susceptible locus at 11q14.1 [6] and 5p15 [7], while studies of Caucasians revealed myopia-susceptibility loci on chromosome 15 [8,9]. We demonstrated the association of these susceptibility loci on chromosome 15 with high myopia in Japanese [10], and a Chinese study successfully replicated the association between high myopia and the *catenin δ2* (*CTNND2*) gene polymorphism in the susceptibility loci 5p15 we determined [11]. However, although the C allele of *CTNND2* single nucleotide polymorphism (SNP) rs6885224 was a risk allele for high myopia in our study, the replication study showed this allele was protective against high myopia. Since the expression of the catenin δ2 protein is regulated by transcription factor Pax6 [12] and *PAX6* is another myopia-susceptibility gene, *PAX6* and *CTNND2* might cooperatively affect myopia development. Although several studies have examined the association between *PAX6* and myopia, whether *PAX6* is a susceptibility gene for myopia remains controversial [13-20]. To determine whether *PAX6* is associated with high myopia, we conducted a large-cohort case–control study of Japanese participants.

Correspondence to: Kenji Yamashiro, Department of Ophthalmology and Visual Sciences, Kyoto University Graduate School of Medicine, 54 Kawahara, Shogoin, Sakyo, Kyoto 606-8507, Japan; Phone: +81-75-752-0933; FAX: +81-75-752-0933; email: yamashro@kuhp.kyoto-u.ac.jp

METHODS

All procedures adhered to the tenets of the Declaration of Helsinki. The Institutional Review Board and the Ethics Committee of each participating institute approved the protocols. All the patients were fully informed of the purpose and procedures of the study, and written consent was obtained from each patient.

Patients and control subjects: In total, 1,307 unrelated Japanese patients with high myopia from the Kyoto University Hospital, Tokyo Medical and Dental University Hospital, Fukushima Medical University Hospital, Kobe City Medical Center General Hospital, and Ozaki Eye Hospital were included in the study. Comprehensive ophthalmic examinations were conducted on all the patients, which included dilated indirect and contact lens slit-lamp biomicroscopies, automatic objective refractions, and measurements of axial length using applanation A-scan ultrasonography or partial coherence interferometry (IOLMaster; Carl Zeiss Meditec, Dublin, CA). An axial length of at least 26 mm in both eyes confirmed the patient had high myopia.

Two control cohorts were recruited for this study. The first cohort was categorized as the selected control group, and comprised 333 cataract patients with axial lengths of less than 25.0 mm in both eyes (control 1). These patients were recruited from the Department of Ophthalmology at Kyoto University Hospital, the Ozaki Eye Hospital, the Japanese Red Cross Otsu Hospital, and the Nagahama City Hospital. In this group, the mean age ± standard deviation (SD) was 75.2±7.9 years; 37.2% were men, and 59.5% were women. Axial length was measured with applanation A-scan ultrasonography or partial coherence interferometry before cataract surgery, and post-surgery, a dilated fundus examination was performed. If the fundus examination revealed that myopic changes had occurred, such as lacquer cracks/peripapillary atrophy, staphyloma, or choroidal neovascularization, the subject was eliminated from the group.

The second cohort was recruited as a general-population control. In total, 923 healthy unrelated Japanese individuals were recruited from the Aichi Cancer Center Research Institute (control 2). Only individuals at least 35 years of age were selected to participate in this group, meaning that the controls were age-matched with the high-myopia cohort. The mean age ± SD of this cohort was 56.9±11.4 years (p=0.855 compared with the high-myopia cohort); 39.3% were men, and 60.7% were women.

Genotyping and statistical analyses: Genomic DNAs were prepared from peripheral blood using a DNA extraction kit (QuickGene-610L; Fujifilm, Minato, Tokyo, Japan) according to the manufacturer's protocol, and the A260/A280 optical density was measured. Extracted DNA was stored at -80 °C until used. Three tag SNPs (rs2071754, rs644242, and rs3026354) were selected using Tagger software, and provided 100% coverage for all common phase II HapMap SNPs (minor allele frequency: >10%; Build: 36.1) within a 22.4-kb region that covered the *PAX6* gene on chromosome 11 (r^2 threshold: 0.90). The samples from patients with high myopia and the cataract controls were genotyped using a commercially available assay (TaqMan SNP assay with the ABI PRISM 7700 system; Applied Biosystems, Foster City, CA). The individuals recruited from the Aichi Cancer Center Research Institute were genotyped using Illumina HumanHap 610 Chips (Illumina Inc., San Diego, CA). The genotype for rs3026354 was obtained from imputed data using MACH software because it was not included in the Illumina BeadChip. Phase II HapMap (Build: 36.1) was referred to for reference sequences.

Deviations from the Hardy–Weinberg equilibrium (HWE) in genotype distributions were assessed for each group using the HWE exact test. The chi-square test for trend or its exact counterpart was used to compare the genotype distributions of the two groups. Multiple regression and logistic regression analysis were performed to adjust for age and sex. These statistical analyses were conducted using Software R (R Foundation for Statistical Computing, Vienna, Austria). A p value of less than or equal to 0.05 was considered statistically significant. Bonferroni correction was used for multiple comparisons.

RESULTS

The demographics of the study population are shown in Table 1. The mean axial length of the 2,614 eyes with high myopia was 29.17±1.84 mm. Of the eyes in this group, 1,878 (71.8%) were phakic, with a mean refraction of −12.71±4.57 D. In the control 1 group, the mean axial length of the 666 eyes was 22.87±0.80 mm, and the mean refraction of the phakic eyes in this group was −0.355±2.96 D.

The genotype counts, associations, and odds ratios (ORs) for the three SNPs in the high-myopia and control groups are shown in Table 2. The genotype distributions of the three SNPs were in HWE (p>0.05). After corrections for age and sex differences had been made, based on a logistic regression model, rs644242 showed a marginal association (p=0.026) with high myopia when evaluated with control 1 (n=333), and a significant association (p=0.015) when evaluated with control 2 (n=923); further analysis demonstrated that this association was still significant after Bonferroni correction. For the high-myopia group, the odds ratios were 0.69 (95%

TABLE 1. CHARACTERISTICS OF THE STUDY POPULATION.

Population characteristics	High myopia*	Case		Control	
		Control 1†	P value	Control 2	P value
Patients (n)	1307	333		923	
Age (mean±SD; years)	57.1±15.0	75.2±7.9	<0.0001‡	56.9±11.4	0.8549‡
Sex (n)					
Male	427 (32.7%)	124 (37.2%)	0.05626§	363 (39.3%)	0.0015§
Female	879 (67.3%)	198 (59.5%)		560 (60.7%)	
Axial length (mm±SD)					
Right eyes	29.23±1.85	22.84±0.81	NA		
Left eyes	29.10±1.82	22.88±0.78	NA		
Refraction of the phakic eyes (D)					
Right eyes	−12.86±4.44	−0.411±3.15	NA		
Left eyes	−12.57±4.71	−0.296±2.77	NA		

* Axial length >26.00 mm in both eyes. † Individuals who underwent cataract surgery and who had an axial length of <25.00 mm in both eyes.‡ Unpaired t test. Compared with the high-myopia group. § Chi-square test. Compared with the high-myopia group. SD: standard deviation, D: diopter, NA: Not applicable.

confidence interval [CI]: 0.49–0.96) for the rs644242 A allele when evaluated with control 1, and 0.79 (95% CI: 0.66–0.96) when evaluated with control 2. Chi-square tests for the trend also showed that rs644242 was significantly associated with high myopia when this group was evaluated with control 2 (p=0.015). The two other SNPs did not have any significant associations with the condition.

Since the allele frequency and the genotype frequency of the three SNPs were not significantly different (p>0.20) between control 1 and control 2, we pooled the controls for further analysis (Table 3). The genotype distributions in the pooled control were still within HWE. This analysis revealed that the rs644242 polymorphism was strongly associated with high myopia. The p value of a chi-square test for the trend was 0.011, and was 0.0045 after adjusting for age and sex with a logistic regression model. Since previous studies have reported on SNP associations with extreme myopia, the genotype distributions of the three SNPs between the extreme myopia cases were compared (axial length ≥28 mm in both eyes) as a pooled control. After age and sex adjustment and Bonferroni correction, this analysis also showed a significant association between rs644242 and extreme myopia (p=0.0165). The OR of this analysis was similar to the OR for the high-myopia analysis (0.78 [95% CI:0.64–0.95]). To investigate whether there are more appropriate genetic association models, we applied other possible ones: dominant, recessive, and codominant. However, we did not find a more significant association than the additive model.

Comparisons between the results of the current study and those of previous studies are summarized in Table 4. The current study is the first study to prove significant associations between a *PAX6* SNP and high myopia and extreme myopia.

DISCUSSION

In the present study, using a relatively large cohort of 2,563 individuals, we showed that *PAX6* is associated with high and extreme myopia in Japanese. The minor A allele of rs644242 was a protective allele for high and extreme myopia.

The association of *PAX6* with common myopia was first evaluated in a Caucasian cohort. Although genome-wide linkage scans in a twins study suggested the *PAX6* region was strongly linked to common myopia, further case–control studies using tag SNPs rejected the hypothesis of an association between *PAX6* and common myopia [13-15]. Regarding high myopia, although Han et al., in a Chinese nuclear family study, reported that two SNPs in *PAX6* were associated with the condition [17], the subsequent case–control study did not replicate these associations, while haplotype analyses using 16 SNPs revealed the association [19]. Two Chinese reports also denied an association of *PAX6* with high myopia, while the subgroup analysis showed *PAX6* was associated with extreme myopia [16,20]. However, only 67 and 55 cases were used in these subgroup analyses, respectively, and therefore, caution should be applied when interpreting the findings, as pointed out by Zayats et al. [21].

Table 2. Genotype counts, associations, and odds ratios in participants with high myopia and control participants.

Single nucleotide polymorphisms	Genotype	High myopia	Control 1				Control 2			
		n	n	Nominal p value*	Adjusted p value†	Adjusted OR (95% CI)	n	Nominal p value*	Adjusted P value†	Adjusted OR (95% CI)
rs2071754 (C/T)	CC	326	90	0.61	0.26	1.12 (0.92-1.38)	232	0.485	0.497	1.04 (0.93-1.17)
	CT	632	156				466			
	TT	344	87				225			
rs644242 (C/A)	CC	1052	258	0.12	0.026	0.69 (0.49-0.96)	710	0.0153	0.0152	0.79 (0.66-0.96)
	CA	237	68				195			
	AA	14	7				18			
rs3026354 (A/G)	AA	544	142	0.33	0.78	1.03 (0.83-1.29)	376	0.611	0.638	0.97 (0.86-1.10)
	AG	590	155				421			
	GG	171	34				126			

* Differences in the observed genotypic distribution were examined by a chi-square test for trend. † Age and sex adjustment were performed based on a logistic regression model. CI: Confidence interval, OR: Odds ratio.